Fries Rearrangement of Aryl Formates Promoted by BCl_3. Mechanistic Evidence from ^{11}B NMR Spectra and DFT Calculations*

Alessandro Bagno[a], Willi Kantlehner[b], Ralf Kreß[b], and Giacomo Saielli[c]

[a] Department of Chemistry, University of Padova, via Marzolo 1, I-35131 Padova (Italy)
[b] Institut für Organische Chemie der Universität Stuttgart, Pfaffenwaldring 55, D-70569 Stuttgart (Germany)
[c] Institute of Membrane Technology-CNR, Padova Section, via Marzolo 1, I-35131 Padova (Italy)

Reprint requests to Prof. Alessandro Bagno. Fax: +39 0498275239.
E-mail: alessandro.bagno@unipd.it
or Prof. Dr. Willi Kantlehner. Fax: +49 07361 576250. E-mail: willi.kantlehner@fh-aalen.de

Z. Naturforsch. **59b,** 386 – 397 (2004); received January 7, 2004

The Fries rearrangement of model aryl formate esters, promoted by boron trichloride, has been investigated by means of NMR spectroscopy (both experimental and computational) and by DFT calculations. Firstly, the ^{11}B NMR chemical shifts of a series of model boron compounds have been predicted by GIAO-B3LYP/6-31G(d,p) calculations, in order to make predictions of the chemical shifts of transient reaction intermediates observable by ^{11}B NMR. Such ^{11}B spectra for the reaction of two esters (phenyl and 3-methyoxyphenyl formates) have been obtained, and are found to follow different patterns which can be rationalized on the basis of computed chemical shifts. Secondly, DFT calculations (B3LYP/6-31G(d,p) level) have been employed to investigate several mechanistic pathways of the rearrangement of phenyl formate. It is found that the pathways leading to the lowest activation energies are those in which formyl chloride is generated from a complex between phenyl formate and BCl_3, which then acts as the formylating agent.

Key words: Fries Rearrangement, Reaction Mechanisms, Electrophilic Reactions, DFT Calculations, ^{11}B NMR

Introduction

The Fries rearrangement transforms an aryl ester into an *ortho*- or *para*-hydroxycarbonyl compound with Lewis-acid catalysis, thus providing a convenient route to obtain aromatic ketones [1]. Standard catalysts are aluminum chloride or boron trifluoride. The high preparative value of this reaction render this reaction an attractive path, for which there is continuing interest, as attested by several reviews, the most recent one dated 1992 [2].

As can be seen from the number of papers which appeared during the last years, the Fries rearrangement is still a fascinating object of investigation for organic chemists. Thus, a wide variety of catalysts such as polyphosphoric acid [3], methanesulfonic acid/$POCl_3$ [4], montmorillonite clays [5], hafnium trifluoromethanesulfonate [6], scandium trifluoromethanesulfonate [7], zirconium tetrachloride [8] and titanium tetrachloride [9] have all been used to induce the rearrangement. Novel reaction methodologies have also been applied; Fries rearrangements have also been performed under microwave irradiation [10] or in ionic liquids [11].

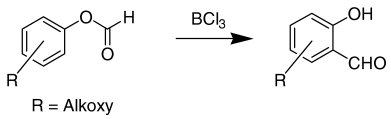

Scheme 1. Fries rearrangement of aryl formates.

Extending the Fries rearrangement to aryl formates is particularly attractive, since it would enable one to introduce a valuable aldehyde functionality. Although the first attempts at doing so (using BF_3, HF, polyphosphoric acid or $AlCl_3$) failed [12 – 14], it was recently demonstrated that alkoxyaryl formates can be rearranged according to Fries giving alkoxy-hydroxy-substituted benzaldehydes, if Lewis acids (such as

* Presented in part at the 6th Conference on Iminium Salts (ImSaT-6), Stimpfach-Rechenberg (Germany), September 16 – 18, 2003.

boron trichloride or boron tribromide) or superacids (such as trifluoromethanesulfonic acid) are used as catalysts (Scheme 1) [15].

Despite several studies, no satisfactory and comprehensive mechanistic picture for this reaction has emerged, also owing to the variety of combinations of substrate and catalyst that have been adopted [1]. There is consensus that the reaction proceeds through a 1:1 (or possibly 1:2 [16]) adduct with the Lewis acid catalyst, and that the carbonyl functionality is introduced through a Friedel-Crafts acylation, presumably *via* an acylium ion intermediate [1]. With CF_3SO_3H as catalyst, the reaction is known to be reversible [17]. However, other major mechanistic features are not well established. Thus, the rearrangement has been claimed to be: (a) intermolecular for both the *ortho* and *para* isomers [18]; (b) intramolecular (at least for the *ortho* isomer) [19], or (c) both (albeit in a polymeric substrate system) [20].

In any event, there is little knowledge concerning the detailed steps of each mechanistic proposal. Thus, most studies broadly agree on a picture where an unspecified complex between substrate and Lewis acid undergoes a dissociative (rather than concerted) pathway, whereby an acylium cation (or acyl chloride) is expelled and subsequently acts as acylating agent [16–20]. On the other hand, a π complex between the acylium ion and the aromatic substrate has been proposed to account for the observed intramolecular process [19].

These circumstances have prompted us to pursue this topic from two novel viewpoints. Thus, we built on previous experimental results pertaining to the Fries rearrangement promoted by boron trichloride, as follows [15]. On one hand, we obtained ^{11}B NMR spectra during the reaction course and attempted to understand the ^{11}B spectra of reaction intermediates through the comparison with chemical shifts calculated by density functional theory (DFT). On the other hand, we investigated a variety of viable reaction mechanisms, again by DFT calculations, in order to clarify some mechanistic issues.

Experimental and Computational Section

Aryl formates and BCl_3 (heptane solution) were commercial. The samples were prepared by rapidly mixing the aryl formate and the BCl_3 solution so as to attain a 1:1 molar mixture in heptane. ^1H and ^{11}B NMR spectra were obtained on a Bruker Avance DRX 400 instrument operating at 9.4 T (400.13 MHz for ^1H, 128.38 MHz for ^{11}B) at the specified temperatures. The measurements were run without lock in 5-mm tubes, which was allowed for by the magnet stability and very short measuring times. For ^{11}B NMR, the following main parameters were adopted: $\pi/2$ pulse 26.5 μs, spectral window 12 kHz, relaxation delay 1 ms. The combination of high sensitivity of ^{11}B and its relatively fast relaxation allowed to obtain spectra with an excellent *S/N* ratio in a matter of 2 – 3 minutes.

DFT calculations of structures, energies and nuclear shieldings were carried out with *Gaussian 98* [21] at the specified levels of theory, except relativistic calculations on some boron calibration compounds (see Results) which were performed with the *ADF* [22] package.

Results and Discussion

Esters [R–C(O)–OR'] possess two sites capable of acting as a Lewis base, *i.e.* the oxygen of the alcohol residue (–**O**R') and the acyl oxygen, R–C(**O**). Thus, in principle BCl_3 may bind to the formate ester in each of the following ways (*O*-aryl or *O*-acyl complexation, Scheme 2):

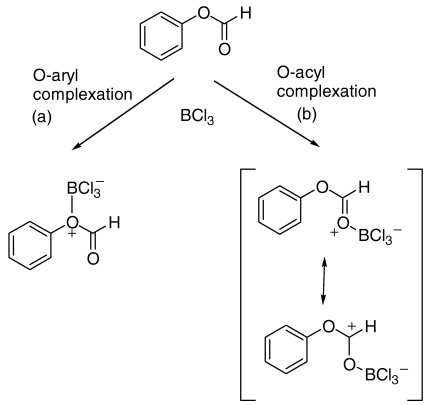

Scheme 2. Possible complexation modes of phenyl formate with boron trichloride.

A straightforward way to represent the initial stage (addition of the Lewis acid) is *O*-aryl complexation (a). However, calculations of the protonation site of formic acid and methyl formate have shown that *O*-aryl protonation is not only much less favorable energetically than *O*-acyl protonation, but also leads essentially to C–O fission and to a loose complex between water (or alcohol) and the acylium cation [23]. Since BCl_3 complexation is a qualitatively similar phenomenon, the energetics of this reaction should be investigated, and mechanisms involving both *O*-aryl and *O*-acyl com-

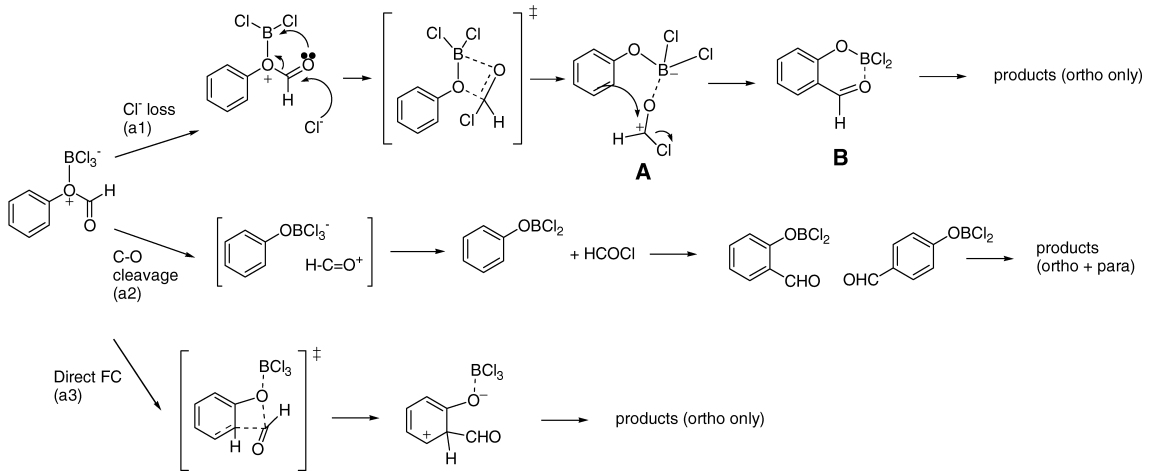

Scheme 3. Proposed mechanistic pathways for the *O*-aryl complex.

plexation should be considered. A mechanistic spectrum may then be proposed as follows. The *O*-aryl (a) and *O*-acyl (b) complexes may react as sketched in Schemes 3 and 4, respectively, which will be examined in turn.

Path (a): O-Aryl complex

Path *(a1)* postulates an initial loss of Cl^- from the adduct (see Scheme 3). Subsequent readdition to the carbonyl group may trigger a rearrangement to yield the intermediate **A**, which eventually undergoes an intramolecular Friedel-Crafts acylation leading to the aryl-dichloroborate **B** and is eventually hydrolyzed to the final product. (Indeed, for the purposes of this work **B** can be viewed as the product since its hydrolysis will not be rate-determining). The transition state (TS) leading to **A** is a four-membered ring, and as such it is expected to be relatively unfavorable. Path *(a2)* envisions the formation of a "free" formylium cation through C–O cleavage, whereby the corresponding *para* isomer **B** may also form. However, the high energy of HCO^+ calls for some caution in invoking its intermediacy. It might also be argued that the actual electrophilic species is formyl chloride, HCOCl. Finally, there might be a direct intramolecular Friedel-Crafts (FC) acylation where the electrophile is the incipient formylium ion *(a3)*. Again, this path involves a strained cyclic TS; however, *O*-aryl complexation might involve lengthening of the C–O bond (see above), which might lead to increased reactivity.

Path (b): O-Acyl complex

Path *(b1)* involves an initial loss of Cl^- from the adduct, its readdition with rearrangement with the formation of the intermediate **C**, proceeding to **B** as seen before through **A** (see Scheme 4). Once again, the rearrangement step requires a 4-membered cyclic TS. Alternatively, Cl^- may recombine with the substrate to give rise to the neutral intermediate **D** (a chloroalkyl-dichloroborate) before undergoing the rearrangement *(b2)*. A further mechanism, which avoids a strained TS, is represented in *(b3)*: intermediate **D** adds to a further substrate molecule *via* its aryl oxygen, and a phenyl formate molecule is exchanged *via* a 6-membered cyclic TS, yielding again **A**. Finally, one can consider path *(b4)*, similar to *(a3)*, where a direct FC acylation takes place.

A few general and speculative remarks can be given at this point. (1) Both types of BCl_3 complexation can, in principle, account for the products, cfr. *(a1)* and *(b1-4)*. (2) In many cases, a 4-membered cyclic TS, as well as substantial conformational changes, must be involved. Even though such processes may be favorable entropically, the viability of these strained species remains questionable and should be assessed. (3) In paths *(a1)*, *(a3)*, *(b1-4)* the electrophilic center is not separated from the aromatic ring (regardless of whether Cl^- exchange is intermolecular); hence, only *ortho* products are expected. (4) Path *(b3)* is a transformylation from another ester molecule. It requires initial complexation *via* the aryl oxygen, features a 6-membered cyclic TS and hence may be much

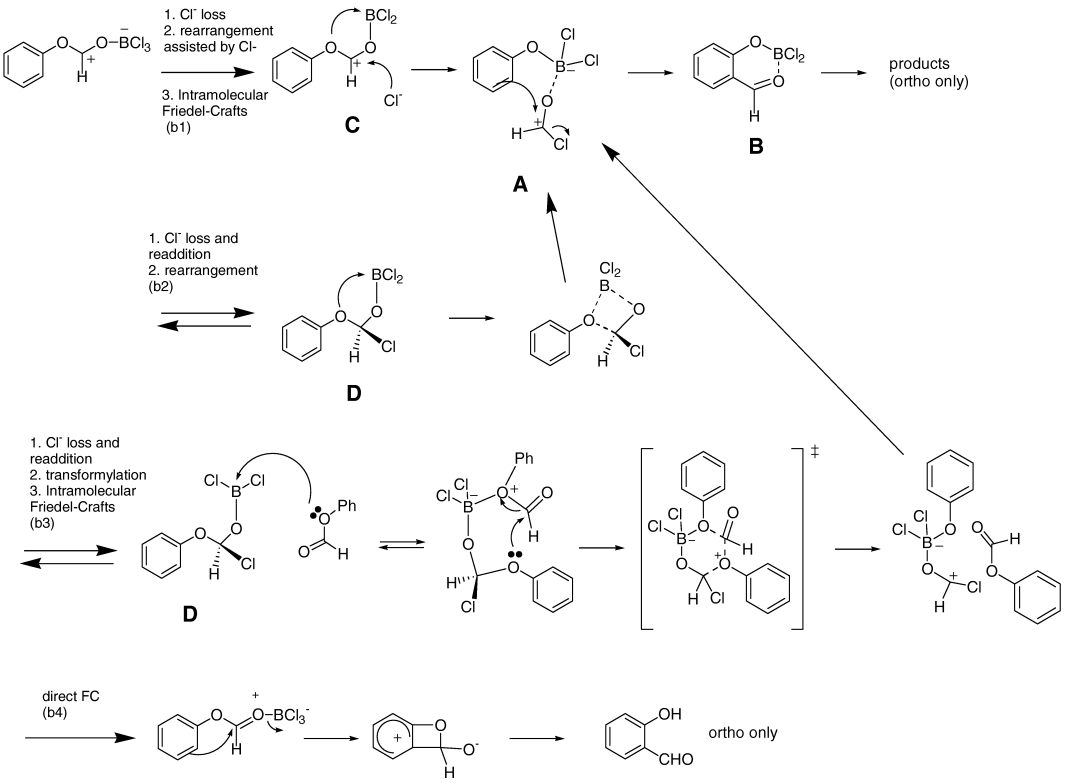

Scheme 4. Proposed mechanistic pathways for the *O*-acyl complex.

less strained. (5) Path *(a2)* leads to a loose complex between Ph–$OBCl_3^-$ and a formylium cation. Chloride abstraction might lead to HCOCl, which may be the actual formylating agent. In this case, *para* acylation may take place. However, the existence of the free formylium cation is very uncertain, and its lifetime is probably too short to act as formylating reagent. Hence, the free formylium ion should not, if possible, be invoked as an intermediate (6). It should be recalled that the boron species envisaged above are only a simplification. In practice, one can expect multiple additions (with corresponding loss of a further chlorine atom).

Guided by these considerations, we have undertaken a combined experimental and theoretical investigation, along the following lines.

We have investigated the ^{11}B NMR chemical shifts of all conceivable intermediates, in connection with the experimental NMR study *via* ^{11}B NMR at low temperature of the addition of BCl_3 to aryl formates, the aim being to distinguish them according to the effect of the different coordination type on the ^{11}B chemical shift. This study involved the comparison between two similar aryl formates showing different reactivity, i. e. phenyl and 3-methoxyphenyl formate, the former being unreactive under the specified conditions (see Introduction).

Furthermore, we have studied the relative stability of *O*-aryl and *O*-acyl complexes of a model substrate (phenyl formate) with BCl_3, the intermediates sketched in Schemes 3 – 4, as well as the potential energy surface (PES) for the major expected pathways, with the aim to characterize major intermediates and transition states.

Structure and energetics of phenyl formate-BCl_3 adducts

This process has been investigated theoretically by DFT methods (B3LYP/6-31G(d,p), with geometry optimization at the same level). Firstly, two conformers of phenyl formate have been located: (a) (planar) and (b) (non-planar), *a* being more stable by 1.6 kcal/mol (Scheme 5).

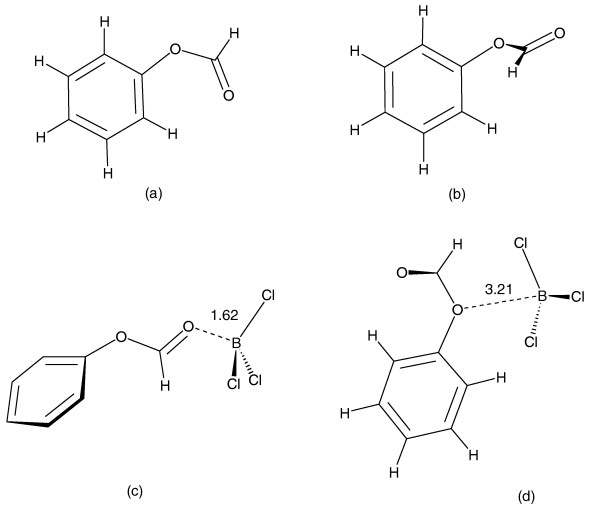

Scheme 5. Structures of phenyl formate and its complexes with BCl_3 (B3LYP/6-31G(d,p) geometry). In (a) and (b) two stable conformers of phenyl formate are represented, whereas (c) and (d) depict the structure of the *O*-acyl and *O*-aryl adducts, respectively.

The structure of the *O*-aryl adduct (Scheme 5d) is that of a loose complex strongly reminiscent of the isolated partners; thus, the B–O distance is very long (3.21 Å), and the BCl_3 moiety retains its planar arrangement. There is, however, a detectable elongation ($\Delta r = 0.01$ Å) of the C(O)–O bond. Overall, it is consistent with the weak energetics of interaction (see below). On the contrary, the *O*-acyl adduct (Scheme 5c) features a fairly short B–O bond (1.62 Å), a substantial lengthening of the C=O bond ($\Delta r = 0.04$ Å), and the BCl_3 moiety takes the expected "tetrahedral" arrangement.

Absolute BCl_3 affinities (ΔE), after correction for the basis-set superposition error (BSSE),[24] show that *O*-aryl complexation is essentially thermoneutral (actually slightly repulsive), whereas *O*-acyl complexation takes place with a stabilization of 28 kcal/mol. (The BSSE correction is essential because absolute energies differ very little otherwise). This is in qualitative agreement with the calculated results for the protonation of formic acid and methyl formate (where relative stabilities differ by *ca.* 20 kcal/mol) [23], or protonation and $AlCl_3$ addition to amides (15–30 kcal/mol) [25]. However, since the *O*-aryl approach is not strongly destabilizing (nor it leads to bond fission like in the case of proton transfer) the *O*-aryl complex may remain a viable intermediate – indeed, it might constitute a *bona fide* activated substrate, whereas the *O*-acyl one might be more stable but kinetically inactive.

Calculation of ^{11}B NMR spectra

The naturally occurring boron isotopes are ^{10}B ($I = 3$, 20%) and ^{11}B ($I = 3/2$, 80%) [26]. The latter is the most frequently used in NMR investigations, owing to its higher receptivity and natural abundance. Since this nuclide possesses an electric quadrupole moment Q, its relaxation is relatively fast and the achievable resolution is only fair. However, since Q is small, line widths are acceptable for many small molecules, thus leading to a series of peaks for each boron species contained in a given sample. Spin-spin coupling may or may not be detectable, depending on various factors [26]; in any event, the kind of species of interest for this work would not exhibit any relevant coupling since boron is directly bonded to O or Cl.

Even though a large number of boron species have been characterized by ^{11}B NMR [26], identification of unstable species by this technique requires an independent evaluation of such NMR spectral parameters, notably the chemical shift. Lately, much progress has been made in this field, and density-functional methods have proved effective at this prediction [27, 28].

Hence, we ran a series of calculations aimed at calibrating the performance of a DFT method for a variety of boron-containing species. These calculations have mostly been carried out with the GIAO-DFT method at the B3LYP/6-31G(d,p) level of theory, for a series of model boron compounds and of proposed reaction intermediates. This relatively small basis set has been chosen in view of the size of the largest molecules to be investigated (triaryl borates). In this framework, the isotropic part of the nuclear shielding tensor σ is made of the two diamagnetic and paramagnetic contributions ($\sigma = \sigma_d + \sigma_p$), and the calculated chemical shift is given by $\delta = \sigma_{ref} - \sigma$, σ_{ref} being the shielding of the reference compound ($BF_3{\cdot}OEt_2$).

Most species relevant to this study contain three chlorine atoms. The direct bonding of heavy atoms to a light one is known to entail marked, and sometimes dramatic, effects on the chemical shift of the light-atom nucleus (*e.g.* the ^{13}C chemical shift of tetraiodomethane at $\delta = -290$ ppm), which are due to relativistic spin-orbit coupling effects [29].

Table 1. Experimental and calculated ^{11}B chemical shifts.[a]

Species	δ_{found}	$\delta_{calcd.}$
Known species:[b]		
BF_3OEt_2	0	0
BH_4^-	−40	−47
BF_4^-	−2.2	−2.4
BCl_4^-	6.6	18
BCl_3	47	50
$PhBCl_2$	55	56
Ph_2BCl	61	72
$B(CH_3)_3$	86	77
Unknown species:[c]		
$MeOBCl_2$		32
o-$C_6H_4(CHO)OBCl_2$[d]		32
$[o\text{-}C_6H_4(CHO)O]_2BCl$[d]		20
$[o\text{-}C_6H_4(CHO)O]_3B$[d]		11
$PhOCH(Cl)OBCl_2$[d]		32
$[PhOCH(Cl)O]_2BCl$[d]		20
$[PhOCH(Cl)O]_3B$[d]		9.8
$PhOCHOBCl_2^+$		40
HCOOPh-BCl_3, *via* acyl O[e]		19
HCOOPh-BCl_3, *via* aryl O[e]		50
$B(OPh)_3$		11
$B(OPh)_2Cl$		19
$B(OPh)Cl_2$		51

[a] Referred to BF_3OEt_2 as standard. $\delta_{calcd.} = \sigma - \sigma_{ref}$; [b] data from ref. [26]; [c] calibration species for which an experimental value is not available; [d] see Scheme 6; [e] see Scheme 5c,d.

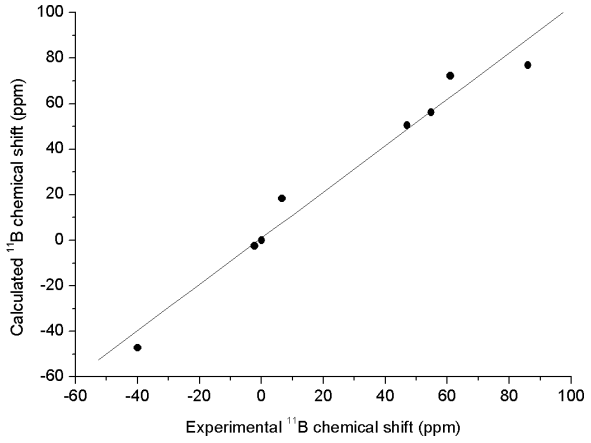

Fig. 1. Correlation between experimental and calculated ^{11}B chemical shifts (data from Table 1). Bromine-containing compounds are excluded since they show major deviations from the correlation (see text). The linear regression has slope 1.01, intercept 0.95 ppm, r = 0.97.

Even though chlorine is a far lighter atom than iodine, similar (if much smaller) effects have been found for ^{13}C in species like dichlorophenols and *o*-bromochlorobenzene [30]. This effect calls for some caution when evaluating these calculated shifts. Therefore, at least a first assessment of relativistic effects on ^{11}B shifts is in order. This check was performed by running calculations at the spin-orbit relativistic ZORA level with a triple-zeta, polarized Slater basis set [22]. In this framework, $\sigma = \sigma_d + \sigma_p + \sigma_{SO}$. The spin-orbit contribution to the ^{11}B shielding (σ_{SO}) turns out to be negligible for non-chlorinated species, small (5 and 8 ppm for BCl_3 and BCl_4^-, respectively) for polychlorinated species, but substantial for brominated species (up to 52 ppm for BBr_4^-). Therefore, keeping in mind the rather low accuracy of chemical shifts, it is not necessary to include this contribution (but it *would* be if one wished to consider BBr_3 as Lewis acid, since the relativistic effect would not be compensated for by the reference), and all further calculations have been carried out at the non-relativistic B3LYP/6-31G(d,p) level. The calibration results (excluding Br compounds) are plotted in Fig. 1, showing that a good accuracy can be attained at this level of theory, considering the relatively low resolution than can be experimentally achieved. Note, however, that the correlation would become much worse for the reasons just discussed if bromine-containing species were included.

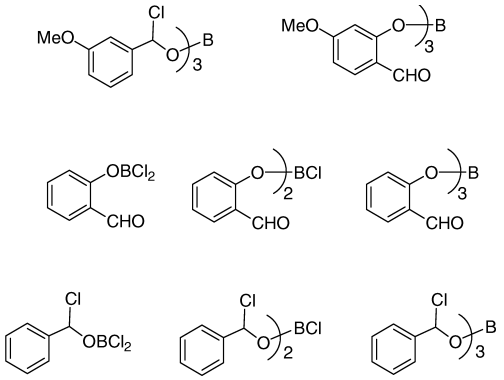

Scheme 6. Proposed key reaction intermediates.

Several species of the type $B(OAr)_mCl_n$ ($m+n=3$) have been calculated (Table 1). The calculated ^{11}B chemical shift of the *O*-aryl complex of phenyl formate is 50 ppm, *i.e.* very close to that of BCl_3 itself, as expected for the very weak interaction already presented (see above). The calculated shift of the *O*-acyl complex is, instead, rather different (19 ppm), *i.e.* well above experimental resolution. Otherwise, all $B(OAr)_mCl_n$ species with the same m and n have very similar shifts, regardless of the structure of the Ar group: $\delta 32 (n=2)$; $\delta 20 (n=1)$; $\delta 10 (n=0)$ (Scheme 6).

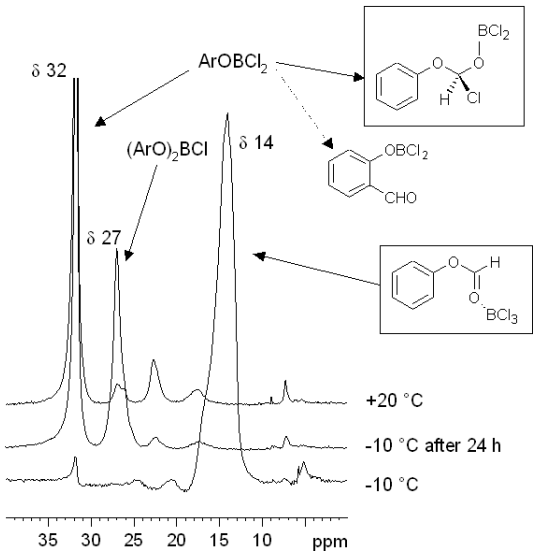

Fig. 2. ^{11}B NMR Spectra of the phenyl formate-BCl_3 mixture. Lower trace: After mixing at -10 °C; middle trace: after 24 h at -10 °C; upper trace: after thawing at 20 °C.

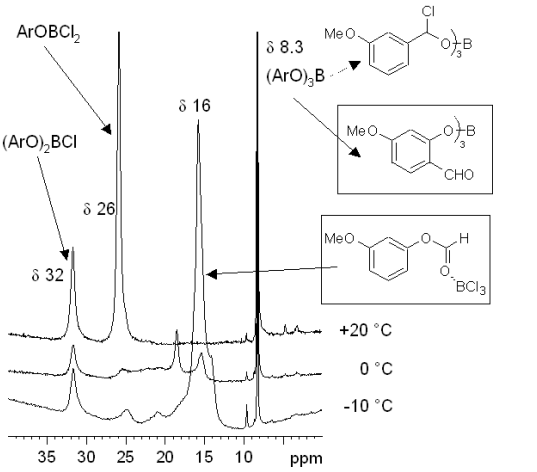

Fig. 3. ^{11}B NMR Spectra of the 3-methoxyphenyl formate-BCl_3 mixture. Lower trace: After mixing at -10 °C; middle trace: 0 °C; upper trace: after thawing at 20 °C.

^{11}B NMR spectra of phenyl and 3-methoxyphenyl formates with BCl_3/heptane

The reaction of phenyl and 3-methoxyphenyl formate with BCl_3 in heptane has been run at low (-10 °C) to room temperature, monitoring its progress by means of ^{11}B NMR spectroscopy (Figures 2–3). ^{11}B spectra were recorded immediately after mixing at -10 °C, and again after letting the sample thaw to 0 °C. A final spectrum was recorded after the sample was allowed to slowly thaw to 20 °C.

No ^{11}B spectrum, even immediately after mixing, shows peaks that can be assigned to "free" BCl_3 ($\delta = 47-50$ ppm), which indicates that the Lewis acid is strongly interacting with the substrate (regardless of whether this interaction causes further reaction or not). Instead, both substrates display a major ^{11}B signal at $\delta = 14-15$ ppm, which (by comparison with the calculations) corresponds to the value for the *O*-acyl complex with BCl_3.

(a) Phenyl formate. Right after mixing, essentially only the peak at $\delta = 14$ ppm is present (Fig. 2). If the sample is left standing at -10 °C for 24 h, the peak at $\delta = 14$ ppm disappears, and is replaced by two additional peaks at $\delta = 27$ and $\delta = 32$ ppm. Upon thawing to 20 °C, the peak at $\delta = 32$ ppm becomes the most prominent one, although some minor peaks between $\delta = 17-27$ ppm are also detectable. This signal is compatible with both $PhOCH(Cl)OBCl_2$ (**D**) and the rearranged intermediate **B**, *o*-$C_6H_4(CHO)OBCl_2$. Since, however, the reaction does not actually proceed with phenyl formate, only the first option is consistent with the results. Hence, presumably the final product from this unreactive ester is $PhOCH(Cl)OBCl_2$ (**D**). The signal observed at $\delta = 27$ ppm at low temperature may be an $(ArO)_2BCl$ species (estimated at $\delta = 20$ ppm, Table 1).

(b) 3-Methoxyphenyl formate. The spectrum (Fig. 3) initially shows again a major peak at $\delta = 16$ ppm (again, presumably, the *O*-acyl complex) and a fairly strong peak at $\delta = 8.3$ ppm. When the sample is allowed to thaw to 0 °C, the peak at $\delta = 8.3$ ppm becomes the main signal, but is accompanied by rather weak ones at $\delta = 15$ (*O*-acyl complex), 18 (not assigned) and 32 ppm (**B** or **D**). When further thawed to 20 °C, the the peak at $\delta = 8.3$ ppm remains the strongest signal, with minor ones at $\delta = 26$ and 32 ppm. Upon standing at room temperature, the latter two signals disappear and only the one at $\delta = 8.3$ ppm remains. Its chemical shift lies in a range typical of trialkyl- or triaryloxyborates like [3-OMe–C_6H_4–$CH(Cl)O]_3B$ or [3-OMe–$C_6H_3(CHO)O]_3B$ (Scheme 6). Since the Fries rearrangement actually proceeds, the peak at $\delta = 8.3$ ppm may be assigned to the rearranged intermediate.

Thus, these data indicate that the two substrates react rather differently with BCl_3; only in the latter case

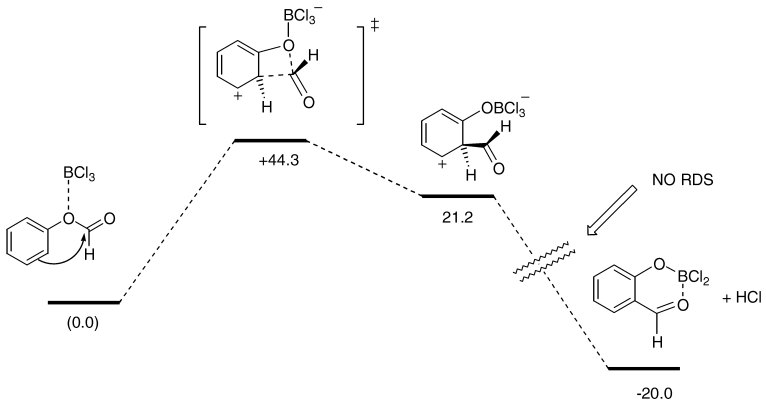

Fig. 4. Potential energy surface for the intramolecular Friedel-Crafts acylation from the *O*-aryl complex, path *(a3)*. The step marked as "NO RDS" is assumed to be not rate-determining.

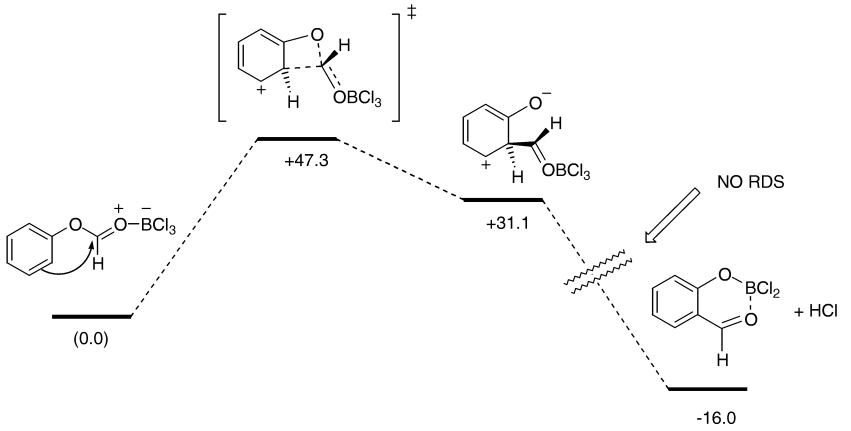

Fig. 5. Potential energy surface for the intramolecular Friedel-Crafts acylation from the *O*-acyl complex, path *(b4)*. The step marked as "NO RDS" is assumed to be not rate-determining.

BCl_3 adds three molecules of aryl formate, and the formation of these intermediates marks the progress of the reaction. Unfortunately, however, ^{11}B NMR cannot discriminate between unrearranged and rearranged intermediate.

DFT study of the mechanism of Fries rearrangement

All calculations were carried out at the B3LYP/6-31G(d,p) level. The geometry of all reactants, transition states, intermediates and products were optimized at that level, and the nature of the critical points was verified by vibrational analysis, confirming that the imaginary vibration led in fact to the desired transformation. Transition-state geometries were optimized by means of the Quadratic Synchronous Transit method, but no IRC analysis was performed [21].

All calculations involved phenyl formate as model substrate. It should be remarked at the outset that, since this compound is not reactive, all activation energies should be considered as an upper bound to those of reactive esters, and the results will only serve for a comparison among different mechanistic path-ways.

Direct intramolecular Friedel-Crafts acylation: paths (a3) and (b4). We will start our discussion with the two alternative mechanisms based on an intramolecular Friedel-Crafts acylation (paths *(a3)* and *(b4)* in Schemes 3 and 4). The conversion from the Wheland intermediate to *o*-hydroxybenzaldehyde was assumed to be non-rate-determining, and no TS was searched for this step in both cases.

Complexation of the ester at the aryl oxygen by BCl_3, path *(a3)*, yields the weakly bound complex of Scheme 5d. In the TS, the complexation of the aryl oxygen becomes much stronger (the B–O bond length is 1.51 Å, compared with 3.21 Å in the reactant complex), whereas the C–O(aryl) bond is increased from 1.36 to 2.14 Å. At the same time the C–C(aryl) bond is partially formed in the TS (2.39 Å). The imaginary vibrational mode in the TS represents the shift of the HCO^+ fomylium ion from the aryl O to the C of the benzene ring. The structures and energies of the three stationary states are collected in Fig. 4.

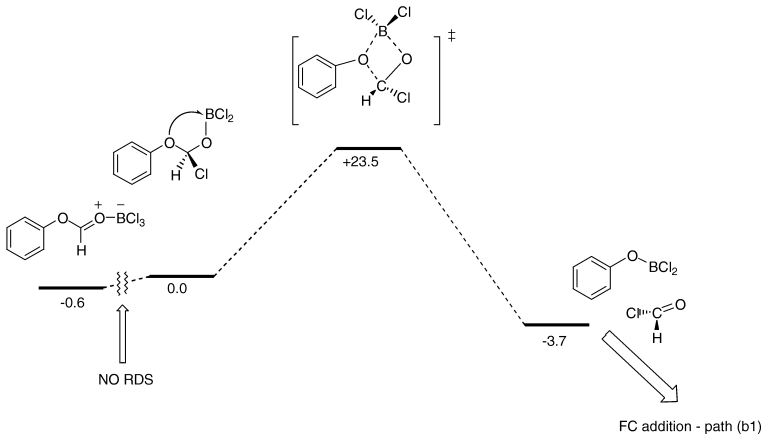

Fig. 6. Potential energy surface for path *(b2)*.

Path *(b4)* is similar to Path *(a3)*: an intramolecular FC acylation takes place, this time starting from the *O*-acyl complex (Scheme 5c). As far as the energetics is concerned, paths *(b4)* and *(a3)* are very similar. However, there is a large difference in the structure of the four-membered ring: for path *(a3)* (complexation at the aryl O), the C–O and C–C bonds are much longer (2.14 and 2.39 Å), while for path *(b4)* (complexation at the acyl O), these bonds are shorter (1.50 and 1.70 Å, respectively). The structures and energies of the three stationary states are collected in Fig. 5.

Friedel-Crafts acylation by HCOCl generated in situ*: paths (b1) and (b2).* Starting from the more stable *O*-acyl complex it is possible to have loss of Cl^- and its subsequent readdition to the carboxyl carbon yielding $PhOCHClOBCl_2$ (**D**). The intramolecular rearrangement with loss of HCOCl is repesented in Fig. 6, path *(b2)*. The breaking C–O bond at the TS is quite elongated (1.87 Å), *i.e.* resembling a weakly bound complex between $PhOBCl_2$ and HCOCl (a product-like TS).

Path *(b2)* can be viewed as the initial stage for the subsequent acylation of $PhOBCl_2$ by HCOCl, which is represented by path *(b1)*. Thus, starting from the complex between $PhOBCl_2$ and HCOCl, the reaction may proceed further through a normal FC addition to the aromatic ring. In principle, this may occur both at the *ortho* and *para* positions, activated by $OBCl_2$ group. The *ortho* addition may be favoured by a stabilizing interaction of the electrophilic B atom with a Cl or O atom of formyl chloride (B···Cl or B···O assisted; see below). Herein, we will only discuss the *ortho* addition.

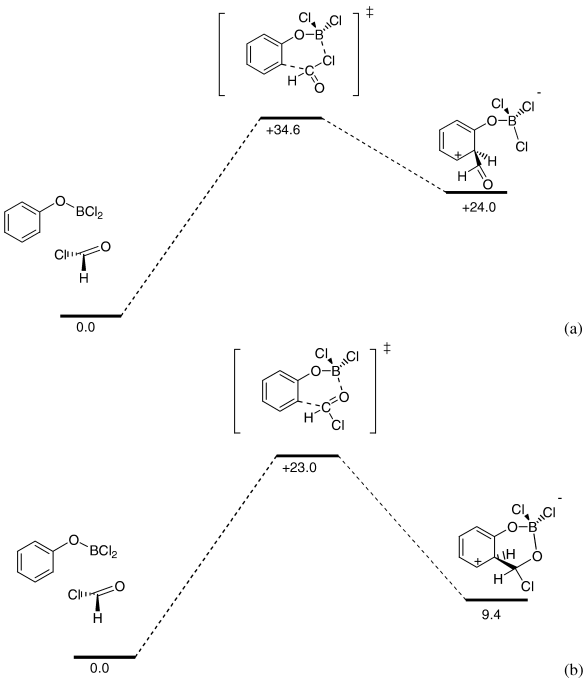

Fig. 7. Potential energy surface for path *(b1)*. (a) B···Cl assisted; (b) B···O assisted.

This electrophilic addition to the ring may itself take place in two ways, *i. e.* through assistance by a chlorine atom (B···Cl assisted), or by an oxygen atom (B···O assisted). Both have been investigated, and the results are presented in Figures 7a – b. In the first case, the resulting Wheland intermediate would directly lead to **B**, whereas in the second one it is the formal adduct of formyl chloride. These TS's also differ in the extent of advancement of electrophilic addition. In the case of B···Cl assistance (Scheme 7a, higher-energy TS),

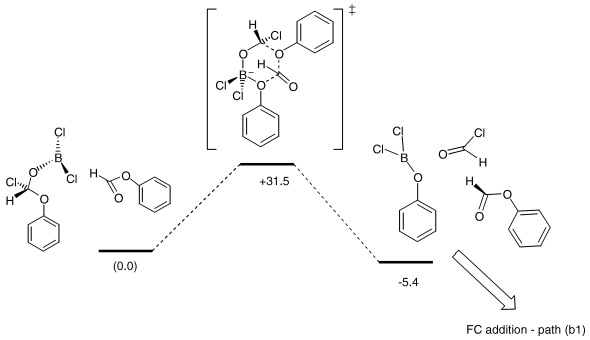

Fig. 8. Potential energy surface for path *(b3)*.

the C–C bond being formed has a length of 2.15 Å with a rather small distortion of the aromatic ring from planarity, whereas in the case of B···O assistance (Scheme 7b, lower-energy TS), the same distance amounts to 2.10 Å and the ring distortion is stronger. Therefore, the latter TS is more product-like.

Transformylation: path (b3). This pathway involves intermediate **D**, which adds a further ester molecule at the aryl oxygen, exchanges a formyl group and falls back to a complex between $PhOBCl_2$ and HCOCl, expelling an ester molecule and presumably entering path *(b1)*; see Fig. 8.

The calculated transition-state structures are collected in Fig. 9.

Of all the pathways examined, paths *(a3)* and *(b4)* are found to exhibit the highest activation barriers ($>$ 40 kcal/mol), consistently with the strained nature of their transition states. Hence, even though from a purely energetical viewpoint they are probably much less favored than the others, such mechanisms might be favored entropically.

On the other hand, pathways *(b2)* and *(b3)*, with lower activation barriers (23 and 31 kcal/mol, respectively), are simply different preparation stages for the subsequent step *(b1)*, in that both pathways represent different modes of generation of formyl chloride as the active electrophile, which eventually acylates $PhOBCl_2$. This step may itself occur in two ways, *i.e.* with assistance from Cl or O (Fig. 7). Since the latter features the smaller activation energy (23 *vs.* 35 kcal/mol) we will assume B···O assistance (Fig. 7b) in the remaining discussion.

In the first case, path *(b2)* envisions the formation of intermediate **D** (Scheme 4) through Cl^- loss and readdition from the *O*-acyl complex; we note that **D** is only marginally higher in energy than its precursor. Interestingly, the activation barrier for its decomposition to $PhOBCl_2$ + HCOCl is much smaller than for paths *(a3)* and *(b4)* despite a superficially similar nature (in both cases a four-membered ring is involved, but in this case all bonds are longer).

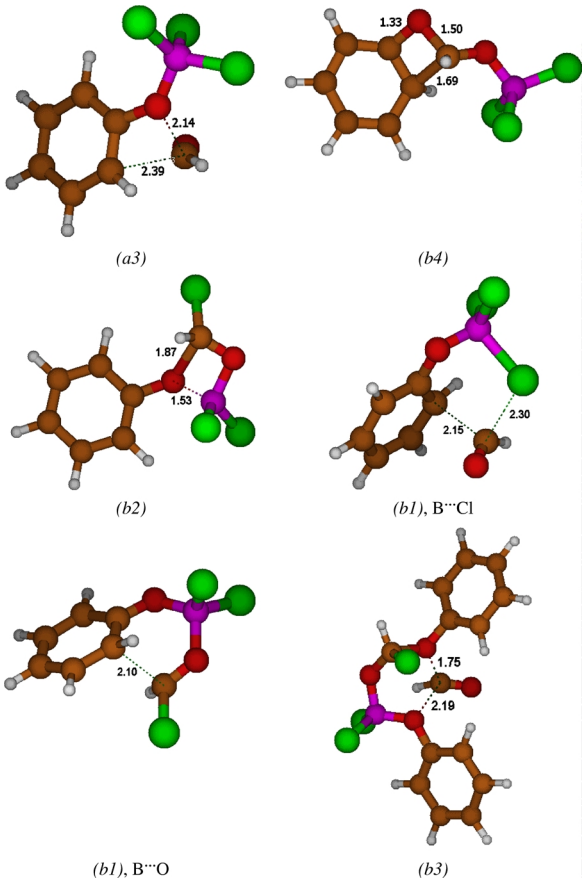

Fig. 9. Calculated structures of the transition states for all mechanisms investigated. Some relevant interatomic distances are given in Å.

The final pathway *(b3)* (transformylation) exhibits a somewhat larger activation energy at 31 kcal/mol; moreover, the complex mode of approach involved may indicate that entropic factors will work against it despite its relatively unstrained geometry. In any event, occurrence of this mechanism might be detected as a different kinetic profile (presumably second-order in ester substrate).

We also note that, of all the TS's determined, only the one for path *(b1)*, B···Cl-assisted, somewhat resembles a π complex between the formylium cation and the aromatic ring, which was suggested as the sta-

blizing factor leading to intramolecular rearrangement [19].

Finally, we recall the work by Hart and coworkers [31], who employed ^{27}Al and ^{17}O NMR to probe the role of $AlBr_4^-$ in the Fries rearrangement of phenyl benzoate promoted by $AlBr_3$. These investigations led to a proposed mechanism where the *O*-acyl complex between PhC(O)OPh and $AlBr_3$ undergoes a C–O(aryl) bond fission mediated by $AlBr_4^-$, leading to a "tight ion pair" [$PhCO^+ \cdot PhOAlBr_3^-$] which would then undergo a pseudo-intramolecular (or "extramolecular") acylation to yield the product with varying *ortho*/*para* ratios. This proposal is essentially similar to path *(b2)* presented herein, although the former requires the explicit intervention of $AlBr_4^-$ (sometimes deliberately added to the reaction mixture) to induce the bond breakage. The corresponding mechanism in our system will be investigated in a further work.

In summary, the current data favor a complex mechanism where the active formylating agent is formyl chloride, generated *in situ* from decomposition of suitable reactive intermediates, paths *(b2)* and *(b3)*. Of course, these results open up the regioselectivity issue, since the intermolecular acylation step might conceivably lead to the *para* substituted product too (see above), which will also be the subject of further work. It should also be noted that the above pathways cannot be sorted out through the analysis of ^{11}B NMR spectra, which however turn out to be a convenient progress monitor for the reaction.

[1] J. March, Advanced Organic Chemistry, 3rd ed., p. 499, Wiley, New York (1985).
[2] R. Martin, Org. Prep. Proced. Int. **24**, 369 (1992).
[3] H. Shargi, E. Eshghi, Bull. Chem. Soc. Jpn. **66**, 135 (1993).
[4] B. Kaboudin, Tetrahedron **55**, 12865 (1999).
[5] C. Venkatachalapathy, K. Pitchumani, Tetrahedron **53**, 17171 (1997).
[6] S. Kobayashi, M. Moriwaki, I. Hachiya, Tetrahedron Lett. **37**, 2053 (1996).
[7] S. Kobayashi, M. Moriwaki, I. Hachiya, J. Chem. Soc., Chem. Commun. 1527 (1995).
[8] D. C. Horrowven, R. R. Dainty, Tetrahedron Lett. **37**, 7659 (1996).
[9] R. Martin, P. Demerseman, Synthesis 25 (1989).
[10] F. M. Moghaddam, M. Ghaffarzadeh, S. H. Abdi-Oskoui, J. Chem. Res. Syn. 574 (1999).
[11] J. R. Harjani, S. J. Narja, M. Salunkhe, Tetrahedron Lett. **42**, 1779 (2001).
[12] D. Kästner, Angew. Chem. **54**, 296 (1941).
[13] G. A. Olah, in G. A. Olah (ed.): Friedel-Crafts and Related Reactions, Vol. I, p. 116, Wiley Interscience, New York (1963).
[14] G. A. Olah, in G. A. Olah (ed.): Friedel-Crafts and Related Reactions, Vol. III/2, p. 1157, 1241, Wiley Interscience, New York (1964).
[15] G. Ziegler, E. Haug, W. Frey, W. Kantlehner, Z. Naturforsch. **56b**, 1178 (2001).
[16] N. M. Cullinane, R. A. Woolhouse, B. F. R. Edwards, J. Chem. Soc. 3842 (1961).
[17] F. Effenberger, R. Gutmann, Chem. Ber. **115**, 1089 (1982).
[18] a) F. Krausz, R. Martin, Bull. Soc. Chim. Fr. 2192 (1965); b) R. Martin, Bull. Soc. Chim. Fr. 983 (1974); c) R. Martin, Bull. Soc. Chim. Fr. II-373 (1979).
[19] Y. Ogata, H. Tabuchi, Tetrahedron **20**, 1661 (1964).
[20] A. Warshawsky, R. Kalir, A. Patchornik, J. Am. Chem. Soc. **100**, 4544 (1978).
[21] Gaussian 98, Revision A.9, M. J. Frisch, G. W. Trucks, H. B. Schlegel, G. E. Scuseria, M. A. Robb, J. R. Cheeseman, V. G. Zakrzewski, J. A. Montgomery (Jr.), R. E. Stratmann, J. C. Burant, S. Dapprich, J. M. Millam, A. D. Daniels, K. N. Kudin, M. C. Strain, O. Farkas, J. Tomasi, V. Barone, M. Cossi, R. Cammi, B. Mennucci, C. Pomelli, C. Adamo, S. Clifford, J. Ochterski, G. A. Petersson, P. Y. Ayala, Q. Cui, K. Morokuma, D. K. Malick, A. D. Rabuck, K. Raghavachari, J. B. Foresman, J. Cioslowski, J. V. Ortiz, A. G. Baboul, B. B. Stefanov, G. Liu, A. Liashenko, P. Piskorz, I. Komaromi, R. Gomperts, R. L. Martin, D. J. Fox, T. Keith, M. A. Al-Laham, C. Y. Peng, A. Nanayakkara, M. Challacombe, P. M. W. Gill, B. Johnson, W. Chen, M. W. Wong, J. L. Andres, C. Gonzalez, M. Head-Gordon, E. S. Replogle, J. A. Pople, Gaussian, Inc., Pittsburgh, PA (1998).
[22] G. te Velde, F. M. Bickelhaupt, E. J. Baerends, C. Fonseca Guerra, S. J. A. van Gisbergen, J. G. Snijders, T. Ziegler, J. Comput. Chem. **22**, 931 (2001), and references cited therein.
[23] A. Bagno, G. Scorrano, J. Phys. Chem. **100**, 1536 (1996).
[24] S. F. Boys, F. Bernardi, Mol. Phys. **19**, 553 (1970).
[25] A. Bagno, W. Kantlehner, O. Scherr, J. Vetter, G. Ziegler, Eur. J. Org. Chem. 2947 (2001).
[26] J. D. Kennedy, in J. Mason (ed.): Multinuclear NMR, p. 221, Plenum Press, New York (1987).
[27] T. Helgaker, M. Jaszunski, K. Ruud, Chem. Rev. **99**, 293 (1999).
[28] T. Onak, J. Jaballas, M. Barfield, J. Am. Chem. Soc. **121**, 2850 (1999).

[29] M. Kaupp, O. L. Malkina, V. G. Malkin, P. Pyykkö, Chem. Eur. J. **4**, 118 (1998).
[30] A. Bagno, F. Rastrelli, G. Saielli, J. Phys. Chem. A **107**, 9964 (2003).
[31] a) I. M. Dawson, J. L. Gibson, L. S. Hart, C. R. Waddington, J. Chem. Soc. Perkin Trans. II 2133 (1989); b) J. L. Gibson, L. S. Hart, J. Chem. Soc. Perkin Trans. 2, 1343 (1991).